

Marshall Plan Report:

Non Abelian Plasma Instabilities

Maximilian Attems
Institute for Theoretical Physics,
Technical University Vienna,
Wiedner Hauptstrasse 8-10,
1040 Vienna, Austria

August 15, 2010

Acknowledgements

First of all, I want to thank Professor Michael Strickland for the invitation to the Gettysburg College, where I had the unique opportunity to consult his expertise on real-time simulations for the Quark-Gluon Plasma. I benefited a lot from his intense supervision and support. Furthermore, the Gettysburg College provided a very fruitful and productive environment for my research on non-Abelian plasma instabilities, which constitutes a major part of my PhD thesis. I am very grateful to the Marshall Plan Foundation for their financial support, as without their grant this essential PhD research visit wouldn't have been possible. I thank my supervisor Professor Anton Rebhan for insightful weekly remote meetings and discussions. I thank Mark Drew, Assistant Editor of the Gettysburg Review, for amazing Michaux woods mountain biking. Last but not least I want to thank Daniel Grumiller for drawing my attention to this special scholarship.

Abstract

Non-Abelian plasma instabilities play a crucial role in the nonequilibrium dynamics of a weakly coupled quark-gluon plasma. The Chromo-Weibel instabilities have been proposed as a possible mechanism for the fast apparent thermalization of the quark-gluon plasma and have been extensively studied in stationary anisotropic plasmas using the so-called hard-loop approximation. The generalization to the HEL (hard-expanding-loop) formalism allows the (numerical) calculation of the time evolution of gluonic mean fields in the more realistic dynamical case of anisotropic expansion.

We wish to study numerically the time evolution of instabilities in an anisotropic Yang-Mills plasma expanding longitudinally. We set up a set of local equations in terms of Yang-Mills potentials and additional fields in the adjoint representation describing long-wavelength colour correlations, which are then discretized on a space-time lattice and a momentum-space cylinder hat.

1 Introduction

1.1 Quark-Gluon Plasma

The *Quark Gluon Plasma* (QGP) [1] is a phase predicted by quantum chromodynamics (QCD), the Standard Model theory of strong interactions, which exists at extremely high temperatures and densities as e.g. shortly after the Big Bang. While quarks and gluons are normally confined within hadrons, in the QGP their degrees of freedom are mostly liberated. Hence, the quark gluon plasma is also called deconfined phase. From the 1970's onward, when high temperature QCD was first addressed, it was assumed that the QGP behaved as a gas of weakly interacting quasiparticles (quarks and gluons). The announcement of the discovery of a new state of matter, the quark gluon plasma (see Figure 1), at the Relativistic Heavy Ion Collider (RHIC) in Brookhaven National Laboratory [2] in the spring of 2005 spurred theoretical research in this area. When a number of collective phenomena, usually present in strongly coupled systems that have short free mean paths, were observed in the new phase it became apparent that the theoretical description of the quark gluon plasma was more subtle than expected.

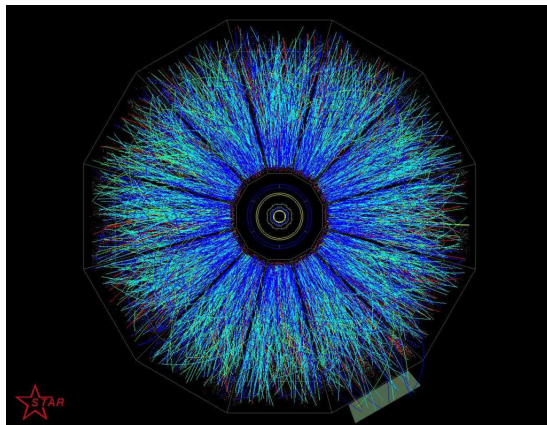


Figure 1: QGP plasma from Au-Au collisions at RHIC

The key question, which has emerged, is whether it is more appropriate to describe this extreme state of matter, that is generated in relativistic heavy ion collisions, by weakly coupled methods or by a strong-coupling formalism. Until today, there is no definitive answer to this question. Hence

both approaches should be studied in order to learn more about weakly and strongly coupled plasma physics and their differences.

Due to asymptotic freedom, the QGP becomes weakly coupled as we go to the theoretically clean limit of very large temperatures T . On the other hand, non-perturbative methods at the critical temperature $T_c \sim 190$ MeV of QCD is out of reach for weakly coupled methods. The important open question, which has to be answered, is thus at which temperature weak-coupling techniques become reliable. The upcoming heavy ion experiments at the Large Hadron Collider (LHC) at the European Laboratory for Particle Physics (CERN) will reach 4-5 times the QCD critical temperature. In this regime, thermodynamic quantities of the quark gluon plasma might already be reliably described by weak-coupling approaches.

One of the most important observations in the QGP produced at RHIC is the phenomenon called *elliptic flow* [3]. It describes the azimuthal momentum space anisotropy of particle emission from non-central heavy-ion collisions in the plane transverse to the beam direction. Since it directly reflects the initial spatial anisotropy of the overlap region of the colliding nuclei in the transverse plane. Because this anisotropy is largest in the beginning of the evolutions it is highly sensitive to the initial conditions. The measurement of elliptic flow is particularly interesting for gaining insight into the thermalization [4] time scale of the plasma. Subsequent to the elliptic flow measurement early thermalization was measured in Au-Au collisions at RHIC. This rapid thermalization means that a thermal state is achieved within a time scale of less than $1 \text{ fm}/c$.

The experimentally measured properties of the quark gluon plasma poses many puzzles. In order to make progress on the description of the QGP we will make use of an effective field theory which incorporates non-equilibrium diagrammatic methods.

The *Hard Thermal Loops (HTL)* effective field theory of QCD is a non-perturbative method, whose numerical simulations can be generalized to analyze dynamics of plasmas far from equilibrium. These simulations provide a method to probe the frontiers of non-equilibrium gauge field theory. A generalized version of the Boltzmann-Vlasov transport equation can be applied for non-stationary anisotropically expanding plasmas while also reproducing the HTL effective action near equilibrium. In a joint collaboration, M. Strickland, A. Rebhan and I have developed a practicable discretization method for real-time simulation in comoving coordinates. This report will

discuss the recent developments in building a C++ code that can simulate non-Abelian plasma instabilities. We show plots of rigorous test cases against 3+1 dimensional fixed box and 1+1 dimensional expanding code.

1.2 Scales of a weakly QGP

A sufficiently small (gauge) coupling g introduces a hierarchy of scales for an ultra-relativistic plasma. In thermal equilibrium, the primary scale is the temperature T , which determines the mean energy of (“hard”) particles in the plasma. The “soft” scale gT with $g \ll 1$ is the scale of thermal masses that determine the plasma frequency, below which no propagating modes exist, the Debye screening mass, and the scale of Landau damping.

When it comes to nonequilibrium physics, it turns out that the parametrically most important phenomena are plasma instabilities [5, 6, 7] that appear already in the collisionless limit, on the level of the HTL masses (and only those of gauge bosons [8]).

1.3 Chromo-Weibel instability

The following picture Fig. 2 of a plasma phenomena from NASA’s Solar Dynamics Observatory shows the complicated structure of QED plasma physics due to the long-ranged electromagnetic interactions. Unlike traditional plasmas, in the QGP it is safe to assume that color magnetic fields cannot exist on distance scales larger than the confinement length. Non-Abelian interactions cause magnetic confinement over distances of order $1/(g^2T)$.

The chromo-Weibel instability arises in non-equilibrium situations where particle momenta are anisotropic in local fluid frames. See Fig. 3 for an illustration of the Weibel instability in a QED plasma. The instability growth rate turns out to be faster than the rate of individual particle collisions. These non-Abelian instabilities create non-perturbatively relatively large magnetic fields. They can thus drive isotropization at rates which are parametrically faster than perturbative scattering rates. Growing instabilities imply that the stress tensor of the non-equilibrium system will receive growing contributions from the soft gauge field. It is important to perform full 3+1 dimensional simulations of the collisionless kinetic theory to verify this behaviours observed in an expanding 1+1 dimensional configuration space ([9],[10]). In the early stages of a relativistic heavy ion collision one expects a non-equilibrium parton system to emerge.

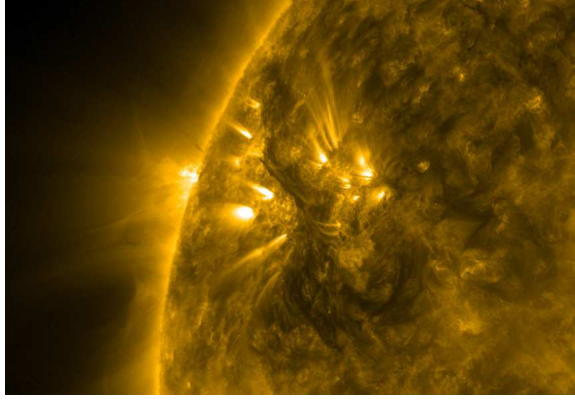


Figure 2: Image of filament and active solar region, taken in extreme UV light from NASA's Solar Dynamics Observatory (May 18, 2010).

2 HEL Equations of motion

The two basic ingredients are the Vlasov equations, which are the collisionless Boltzmann equations for colored perturbations $\delta f_a(\mathbf{p}, \mathbf{x}, t)$ and the non-Abelian Maxwell equations for field strengths $F_a^{\mu\nu}$. Assuming a color neutral background distribution function $f_0(\mathbf{p}, \mathbf{x}, t)$ which satisfies

$$v \cdot \partial f_0(\mathbf{p}, \mathbf{x}, t) = 0, \quad v^\mu = p^\mu / p^0, \quad (1)$$

where v^μ is the four velocity, the Vlasov equations are given by

$$v \cdot D \delta f_a(\mathbf{p}, \mathbf{x}, t) = g v_\mu F_a^{\mu\nu} \partial_\nu^{(p)} f_0(\mathbf{p}, \mathbf{x}, t) \quad . \quad (2)$$

The Maxwell equations for the soft gauge fields are

$$D_\mu F_a^{\mu\nu} = j_a^\nu = g t_R \int \frac{d^3 p}{(2\pi)^3} \frac{p^\nu}{2p^0} \delta f_a(\mathbf{p}, \mathbf{x}, t) \quad . \quad (3)$$

So far, the distribution function was chosen mostly stationary $f_0(\mathbf{p})$ with $\partial_\mu f_0 \equiv 0$. In the thermal (or just isotropic) case, the magnetic term of the Vlasov equation (2) drops out, where as in the anisotropic case magnetic interactions lead to much more complicated and richer dynamics.

- isotropic: $f_0(\mathbf{p}) = f_0(|\mathbf{p}|)$, $\nabla_{\mathbf{p}} f_0 \propto \mathbf{v}$

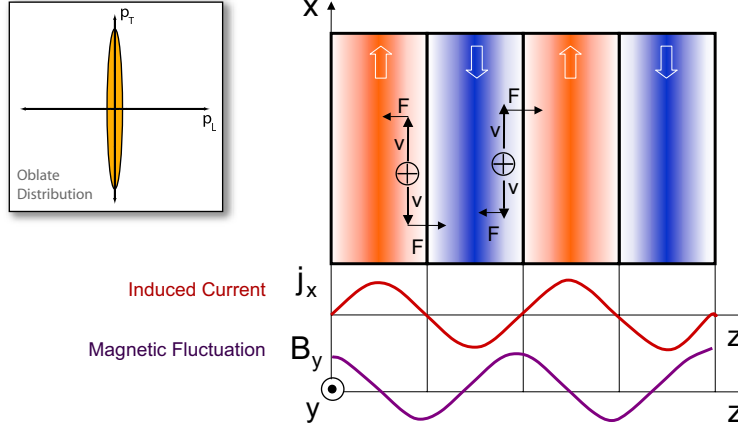


Figure 3: Illustration of the mechanism of filamentation (Weibel) instabilities [11]: Charged plasma particles moving transversely to the wave vector of a seed magnetic field tend to separate in counterstreaming currents which in turn amplify the magnetic field. The upper left corner indicates the momenta anisotropy.

$$v \cdot D \delta f_a(\mathbf{p}, \mathbf{x}, t) = -g \mathbf{E}_a \cdot \nabla_{\mathbf{p}} f_0 \quad (\text{stable}) \quad (4)$$

- anisotropic: $f_0(\mathbf{p}), \nabla_{\mathbf{p}} f_0 \not\propto \mathbf{v}$

$$v \cdot D \delta f_a(\mathbf{p}, \mathbf{x}, t) = -g(\mathbf{E}_a + \mathbf{v} \times \mathbf{B}_a) \cdot \nabla_{\mathbf{p}} f_0 \quad (\text{unstable!}) \quad (5)$$

It has been shown that the HTL effective action can be straightforwardly extended to systems using collisionless gauge-covariant transport field theory [12]. Using an auxiliary field formulation one can carry out a full hard-loop simulation. Factorizing

$$\delta f^a(x; p) = -g W_\mu^a(t, \mathbf{x}; \mathbf{v}) \partial^\mu(p) f_0(\mathbf{p}) \quad (6)$$

one obtains

$$[v \cdot D(A)] W_\mu(x; \mathbf{v}) = F_{\mu\gamma}(A) v^\gamma \quad (7)$$

and

$$D_\sigma(A) F^{\sigma\mu} = j^\mu(x) = \frac{1}{\mathcal{N}} \sum_v v^\mu \mathcal{W}_v(x) \quad (8)$$

where $v^\mu \equiv p^\mu/|\mathbf{p}| = (1, \mathbf{v})$ and \mathcal{W} is an auxiliary field. The accuracy can be systematically improved by increasing \mathcal{N} . The induced current is defined as

$$j^\mu(x) = -g^2 \int \frac{d^3p}{(2\pi)^3} \frac{1}{2|\mathbf{p}|} p^\mu \frac{\partial f(\mathbf{p})}{\partial p^\nu} W^\nu(x; \mathbf{v}), \quad (9)$$

but can be written in the simpler form as seen in equation (8) as only one of the four fields \mathcal{W}^ν participates in the dynamical evolution. For real-time lattice simulation the discretization happens both in configuration and velocity space in so called discretized "disco balls".

For the ultrarelativistic case of an longitudinal expansion it is convenient to switch to comoving coordinates

$$\begin{aligned} t &= \tau \cosh \eta, & \beta &= \tanh \eta, \\ z &= \tau \sinh \eta, & \gamma &= \cosh \eta, \end{aligned} \quad (10)$$

i.e, a coordinate system with nontrivial metric $ds^2 = d\tau^2 - d\mathbf{x}_\perp^2 - \tau^2 d\eta^2$. We introduce the notation

$$\tilde{x}^\alpha = (x^\tau, x^i, x^\eta) = (\tau, x^1, x^2, \eta) \quad (11)$$

with indices from the beginning of the Greek alphabet for these new coordinates. In what follows we shall not deal with space-time covariant derivatives and Christoffel symbols, but write everything in terms of explicit derivatives. In particular the gauge covariant derivative always means $\tilde{D}_\alpha = \tilde{\partial}_\alpha - ig[\tilde{A}_\alpha, \cdot]$. Being a two form (where indices are naturally down), the field strength retains its usual form: $\tilde{F}_{\alpha\beta} = \tilde{\partial}_\alpha \tilde{A}_\beta - \tilde{\partial}_\beta \tilde{A}_\alpha - ig[\tilde{A}_\alpha, \tilde{A}_\beta]$. In addition to space-time rapidity η , we also introduce momentum space rapidity y for the massless particles according to

$$p^\mu = p_\perp (\cosh y, \cos \phi, \sin \phi, \sinh y). \quad (12)$$

$$\text{With } p^\beta \partial_\beta [\partial_{(p)}^\alpha f_0(\mathbf{p}_\perp, p_\eta)] \Big|_{p^\mu = \text{const.}} = 0 \quad (13)$$

we can commute $\mathbf{p} \cdot D$ and thus solve gauge-covariant Vlasov equation in comoving coordinates

$$p \cdot D \delta f_a(\mathbf{p}, \mathbf{x}, t) \Big|_{p^\mu = \text{const.}} = gp^\beta F_{\beta\alpha}^a \partial_{(p)}^\alpha f_a(\mathbf{p}, \mathbf{x}, t). \quad (14)$$

We introduce auxiliary fields $W_\alpha^a(\tau, x^i, \eta; \phi, y)$ similar to the auxiliary field $W^\nu(x, \mathbf{v})$ of the hard-loop formalism

$$\delta f^a(x; p) = -gW_\alpha^a(\tau, x^i, \eta; \phi, y)\partial_{(p)}^\alpha f_0(p_\perp, p_\eta) \quad (15)$$

that obey

$$v \cdot DW_\alpha(\tau, x^i, \eta; \phi, y)\Big|_{\phi, y} = v^\beta F_{\alpha\beta} \quad . \quad (16)$$

Instead of the light-like quantity $v^\mu = p^\mu/p^0$ we define

$$V^\alpha \equiv \frac{p^\alpha}{|\mathbf{p}_\perp|} = \left(\cosh(y - \eta), \cos \phi, \sin \phi, \frac{\sinh(y - \eta)}{\tau} \right). \quad (17)$$

Thus a straight forward calculation yields the time derivative of $W_{\bar{\alpha}}$ yields

$$\partial_\tau W_{\bar{\alpha}} = \frac{1}{\cosh(y - \eta)} (V^{\bar{\beta}} F_{\bar{\alpha}\bar{\beta}} - V^i D_i W_{\bar{\alpha}}) - \frac{\tanh(y - \eta)}{\tau} D_\eta W_{\bar{\alpha}}. \quad (18)$$

The \mathcal{W} -field is defined as

$$\mathcal{W} = V^i W_i - \frac{1}{\tau_{\text{iso}}^2} V_\eta W_\eta, \quad (19)$$

where $V^i = (\cos \phi, \sin \phi)$ and $V_\eta = -\tau \sinh(y - \eta)$.

Using Boltzman Vlasov (1) we get

$$V \cdot D\mathcal{W} = \left(V^i F_{i\tau} + \frac{\tau^2}{\tau_{\text{iso}}^2} V^\eta F_{\eta\tau} \right) V^\tau + V^i V^\eta F_{i\eta} \left(1 - \frac{\tau^2}{\tau_{\text{iso}}^2} \right) \quad (20)$$

and hence the time derivative of the \mathcal{W} -field is

$$\begin{aligned} \partial_\tau \mathcal{W} = & \frac{1}{\cosh(y - \eta)} \left[\left(V^i F_{i\tau} + \frac{\tau^2}{\tau_{\text{iso}}^2} V^\eta F_{\eta\tau} \right) V^\tau \right. \\ & \left. + V^i V^\eta F_{i\eta} \left(1 - \frac{\tau^2}{\tau_{\text{iso}}^2} \right) - V^i D_i \mathcal{W} \right] - \frac{\tanh(y - \eta)}{\tau} D_\eta \mathcal{W}. \end{aligned} \quad (21)$$

To solve them, we adopt the comoving temporal gauge $A^\tau = 0$ and introduce canonical conjugate field momenta for the remaining gauge fields according to

$$\Pi^i \equiv \tau \partial_\tau A_i = \tau F_{\tau i}, \quad \Pi^\eta \equiv \frac{1}{\tau} \partial_\tau A_\eta = \frac{1}{\tau} F_{\tau \eta}. \quad (22)$$

The final expression for the time evolution of \mathcal{W} becomes

$$\begin{aligned} \partial_\tau \mathcal{W} = & -\frac{V^i}{\tau} \Pi^i - \frac{\tau^2 \sinh(y - \eta)}{\tau_{\text{iso}}^2} \Pi^\eta + \\ & + \frac{\tanh(y - \eta)}{\tau} \left[\left(1 - \frac{\tau^2}{\tau_{\text{iso}}^2} \right) V^i F_{i\eta} - D_\eta \mathcal{W} \right] + \frac{1}{\cosh(y - \eta)} V^i D^i \mathcal{W}. \end{aligned} \quad (23)$$

In terms of fields and conjugate momenta, the Yang-Mills equations take the form

$$\tau \partial_\tau \Pi^\eta = j_\eta - D_i F^i{}_\eta, \quad (24)$$

$$\tau^{-1} \partial_\tau \Pi_i = j^i - D_j F^{ji} - D_\eta F^{\eta i}. \quad (25)$$

and the Gauss law constraint

$$\tau j^\tau = D_\eta \Pi^\eta - ig[A^i, \Pi_i]. \quad (26)$$

3 Lattice discretization and numerical results

3.1 Method

For a numerical evaluation of equations (23, 22) we discretize proper time τ starting with finite $\tau_0 > 0$ and time step ϵ . The space-time rapidity coordinate η is made periodic and discrete with N_η points and (dimensionless) spacing a_η covering a rapidity interval $(-N_\eta a/2, N_\eta a/2)$. The spatial lattice spacing transversal to η is given by the dimensionful parameter a with N_\perp sites. The (matrix-valued) fields A^x , A^y , and $\mathcal{W}_{\phi,y}$ are defined on the sites of the 3-dimensional lattice, while the conjugate momenta Π_x , Π_y , and Π^η are defined on the temporal links. We introduce the dimensionless coordinate frame

$$\hat{x} = \frac{x}{a}, \quad \hat{y} = \frac{y}{a}, \quad \hat{\eta} = \eta, \quad \hat{\tau} = \frac{\tau}{a}, \quad \hat{\epsilon} = \frac{\epsilon}{a}. \quad (27)$$

All fields, conjugate momenta, and current are rescaled into dimensionless lattice variables.

$$\begin{aligned} \hat{A}^i &= gaA^i, \quad \hat{A}_\eta = gA_\eta, \quad \hat{\Pi}_i = ga\Pi_i, \quad \hat{\Pi}^\eta = ga^2\Pi^\eta, \\ \hat{\mathcal{W}} &= a\mathcal{W}, \quad \hat{j}^\tau = a^3 j^\tau, \quad \hat{j}^i = a^3 j^i, \quad \hat{j}^\eta = a^4 j^\eta. \end{aligned} \quad (28)$$

From this point on all variables, in this section, can be assumed to be dimensionless lattice variables and we will henceforth drop the “hats” on symbols. The parallel transporters U_i and U_η living on the links are given by

$$U_i(\tau + \epsilon, \mathbf{x}, \eta) = \exp\left(-i\epsilon\tau^{-1}\Pi_i(\tau + \frac{\epsilon}{2}, \mathbf{x}, \eta)\right) U_i(\tau, \mathbf{x}, \eta) \quad (29)$$

and

$$U_\eta(\tau + \epsilon, \mathbf{x}, \eta) = \exp\left(i\epsilon\tau a_\eta \Pi_\eta(\tau + \frac{\epsilon}{2}, \mathbf{x}, \eta)\right) U_\eta(\tau, \mathbf{x}, \eta) \quad . \quad (30)$$

The fields are assumed to be periodic in all directions. The continuum equations of motion are translated into gauge-invariant lattice equations of motion by using standard plaquette and staple operators. The plaquette operator is given by

$$U_{\mu\nu}(x) = U_\mu(x)U_\nu(x + \mu)U_\mu^\dagger(x + \nu)U_\nu^\dagger(x) \quad (31)$$

and the gauge link staple S is defined by

$$S_{\mu\nu}^\dagger(\tau, x) = U_\nu(\tau, x + \mu)U_\mu^\dagger(\tau, x + \nu)U_\nu^\dagger(\tau, x) \quad . \quad (32)$$

Products like $F_{\mu\nu}^2$ which appear in the energy density can also be expressed in terms of plaquette variables. For this application we need two different combinations, $F_{\eta i}^2$ and F_{xy}^2 . These are

$$\text{tr } F_{\eta i}^2 = \frac{2}{a_\eta^2} \left(1 - \frac{1}{N_c} \text{tr} [\text{Re } U_{\eta i}]\right) \quad (33)$$

$$\text{tr } F_{xy}^2 = 2 \left(1 - \frac{1}{N_c} \text{tr} [\text{Re } U_{xy}]\right). \quad (34)$$

In terms of plaquette and staple operators the Yang-Mills update equations are

$$\begin{aligned} \Pi_i(\tau + \frac{\epsilon}{2}, \mathbf{x}, \eta) &= \Pi_i(\tau - \frac{\epsilon}{2}, \mathbf{x}, \eta) + \tau\epsilon \left[j_{\text{avg}}^i(\tau, \mathbf{x}, \eta) \right. \\ &\quad \left. - iN_c \text{tr} \left(\tau^a U_i(\tau, \mathbf{x}) \left(S_{ij\neq i}^\dagger(\tau, \mathbf{x}) + S_{i-j\neq i}^\dagger(\tau, \mathbf{x}) \right) \right) \right. \\ &\quad \left. - i\frac{N_c}{a_\eta^2} \text{tr} \left(\tau^a U_i(\tau, \mathbf{x}) \left(S_{i\eta}^\dagger(\tau, \mathbf{x}) + S_{i-\eta}^\dagger(\tau, \mathbf{x}) \right) \right) \right] \quad (35) \end{aligned}$$

and

$$\begin{aligned} \Pi^\eta(\tau + \frac{\epsilon}{2}, \mathbf{x}, \eta) &= \Pi^\eta(\tau - \frac{\epsilon}{2}, \mathbf{x}, \eta) + \frac{\epsilon}{\tau} \left[-\tau^2 j_{\text{avg}}^\eta(\tau, \mathbf{x}, \eta) \right. \\ &\quad \left. + i \frac{N_c}{a_\eta} \text{tr} \left(\tau^a U_\eta(\tau, \mathbf{x}) \left(S_{\eta i}^\dagger(\tau, \mathbf{x}) + S_{\eta-i}^\dagger(\tau, \mathbf{x}) \right) \right) \right], \end{aligned} \quad (36)$$

with the average currents

$$j_{\text{avg}}^i \equiv \frac{1}{2} \left[j^i(\tau, \mathbf{x}, \eta) + U_i^\dagger(\tau, \mathbf{x}, \eta) j^i(\tau, \mathbf{x} + \hat{e}_i, \eta) U_i(\tau, \mathbf{x}, \eta) \right] \quad (37)$$

and

$$j_{\text{avg}}^\eta \equiv \frac{1}{2} \left[j^\eta(\tau, \mathbf{x}, \eta) + U_\eta^\dagger(\tau, \mathbf{x}, \eta) j^\eta(\tau, \mathbf{x}, \eta + \hat{e}_\eta) U_\eta(\tau, \mathbf{x}, \eta) \right]. \quad (38)$$

To discretize the \overline{W} fields we use a rectangular lattice in ϕ - u space of size $N_\phi \times N_u$ and

$$\phi_n = \frac{2\pi n}{N_\phi} \quad (39)$$

$$u_m = -1 + \frac{2m+1}{N_u}, \quad (40)$$

where $n \in \{0, \dots, N_\phi - 1\}$ and $m \in \{0, \dots, N_u - 1\}$. The update equations for the \overline{W} fields then take the form

$$\begin{aligned} \overline{W}(\tau + \epsilon, \mathbf{x}, \eta; \phi, u) &= \overline{W}(\tau - \epsilon, \mathbf{x}, \eta; \phi, u) + 2\epsilon \left\{ -\sqrt{1-u^2} v^i D_i^S \overline{W} \right. \\ &\quad \left. - \frac{u}{\tau} (D_\eta^S \overline{W} - (1-u^2) \partial_u^S \overline{W}) \right. \\ &\quad \left. + \frac{1}{f(\tau, \tau_{\text{iso}}, u)} \left[\frac{1}{\tau} v^i \Pi_i^{\text{avg}} - \frac{\tau^2}{\tau_{\text{iso}}^2} \frac{u}{\sqrt{1-u^2}} \Pi_{\text{avg}}^\eta \right. \right. \\ &\quad \left. \left. + \frac{u}{\tau} \left(1 - \frac{\tau^2}{\tau_{\text{iso}}^2} \right) v^i F_{i\eta} \right] \right\}, \end{aligned} \quad (41)$$

where $F_{i\eta}$ is computed using plaquettes. D_i^S and D_η^S are symmetric covariant derivatives in the transverse and rapidity directions, respectively

$$D_\eta^S \varphi(\eta) \equiv \frac{U_\eta^\dagger(\eta) \varphi(\eta+1) U_\eta(\eta) - U_\eta(\eta-1) \varphi(\eta-1) U_\eta^\dagger(\eta-1)}{2a_\eta} \quad (42)$$

$$D_i^S \varphi(x_i) \equiv \frac{U_i^\dagger(x_i) \varphi(x_i+1) U_i(x_i) - U_i(x_i-1) \varphi(x_i-1) U_i^\dagger(x_i-1)}{2}, \quad (43)$$

and ∂_u^S is a symmetric derivative in u space

$$\partial^S \varphi(u_m) \equiv \frac{\varphi(u_{m+1}) - \varphi(u_{m-1})}{2\Delta u}, \quad (44)$$

where $\Delta u = 2/N_u$. The conjugate momenta, Π_i^{avg} and Π_{avg}^η , appearing in (41) are averaged both spatially and temporally

$$\begin{aligned} \Pi_i(\tau + \frac{\epsilon}{2}, \mathbf{x}, \eta) &= \Pi_i(\tau - \frac{\epsilon}{2}, \mathbf{x}, \eta) + \tau \epsilon \left[j_{\text{avg}}^i(\tau, \mathbf{x}, \eta) \right. \\ &\quad \left. - i N_c \text{tr} \left(\tau^a U_i(\tau, \mathbf{x}) \left(S_{ij \neq i}^\dagger(\tau, \mathbf{x}) + S_{i-j \neq i}^\dagger(\tau, \mathbf{x}) \right) \right) \right. \\ &\quad \left. - i \frac{N_c}{a_\eta^2} \text{tr} \left(\tau^a U_i(\tau, \mathbf{x}) \left(S_{i\eta}^\dagger(\tau, \mathbf{x}) + S_{i-\eta}^\dagger(\tau, \mathbf{x}) \right) \right) \right] \quad (45) \end{aligned}$$

$$\begin{aligned} \Pi^\eta(\tau + \frac{\epsilon}{2}, \mathbf{x}, \eta) &= \Pi^\eta(\tau - \frac{\epsilon}{2}, \mathbf{x}, \eta) + \frac{\epsilon}{\tau} \left[-\tau^2 j_{\text{avg}}^\eta(\tau, \mathbf{x}, \eta) \right. \\ &\quad \left. + i \frac{N_c}{a_\eta} \text{tr} \left(\tau^a U_\eta(\tau, \mathbf{x}) \left(S_{\eta i}^\dagger(\tau, \mathbf{x}) + S_{\eta-i}^\dagger(\tau, \mathbf{x}) \right) \right) \right] \quad (46) \end{aligned}$$

where we have indicated explicitly the fact that the Π 's live on links (halfway between sites) for clarity. The currents are computed from the \overline{W} fields via

$$j^\tau(\tau, \mathbf{x}, \eta) = -\frac{m_D^2}{N_\phi N_u} \sum_{n,m} (1-u^2)^{-\frac{3}{2}} \overline{W}(\tau, \mathbf{x}, \eta; \phi, u), \quad (47)$$

$$j^i(\tau, \mathbf{x}, \eta) = -\frac{m_D^2}{N_\phi N_u} \sum_{n,m} v^i (1-u^2)^{-1} \overline{W}(\tau, \mathbf{x}, \eta; \phi, u), \quad (48)$$

$$j^\eta(\tau, \mathbf{x}, \eta) = -\frac{m_D^2}{\tau N_\phi N_u} \sum_{n,m} u (1-u^2)^{-\frac{3}{2}} \overline{W}(\tau, \mathbf{x}, \eta; \phi, u), \quad (49)$$

We monitor Gauss' Law by periodically checking

$$\frac{1}{N_\perp^2 N_\eta} \sum_{\mathbf{x}, \eta} \text{tr} \left[\tau j^\tau(\tau, \mathbf{x}, \eta) + D_\eta^S \Pi_{\text{avg}}^\eta(\tau, \mathbf{x}, \eta) - D_i^S \Pi_i^{\text{avg}}(\tau, \mathbf{x}, \eta) \right]^2. \quad (50)$$

We compute the discretized transverse and longitudinal contributions to the field energy density \mathcal{E} via

$$\mathcal{E}_T = \frac{1}{N_\perp^2 N_\eta} \sum_{\mathbf{x}, \eta} \text{tr} \left[\tau^{-2} F_{\eta i}^2 + \tau^{-2} \Pi_i^2 \right], \quad (51)$$

$$\mathcal{E}_L = \frac{1}{N_\perp^2 N_\eta} \sum_{\mathbf{x}, \eta} \text{tr} \left[F_{xy}^2 + (\Pi^\eta)^2 \right], \quad (52)$$

where $\text{tr } F_{\eta i}^2$ and $\text{tr } F_{xy}^2$ are computed using Eqs. (33) and (34). Finally, we initialize our tree-dimensional simulations either with Gaussian random B fields or with a transverse electric field in the longitudinal η or in transverse direction. We can on runtime decide if we are computing an Abelian or non-Abelian setup.

3.2 HEL Testcases

The resulting code got checked in a git repository for version control. The HEL code repository shows 137 commits during the 3 month of stay in Gettysburg college. This means on average 1.5 commit / day. The overall git statistics for the whole stay show 62 files changed with over 3500 line changes.

Figure 4 shows the output of 2 different codebases on top of each other. The

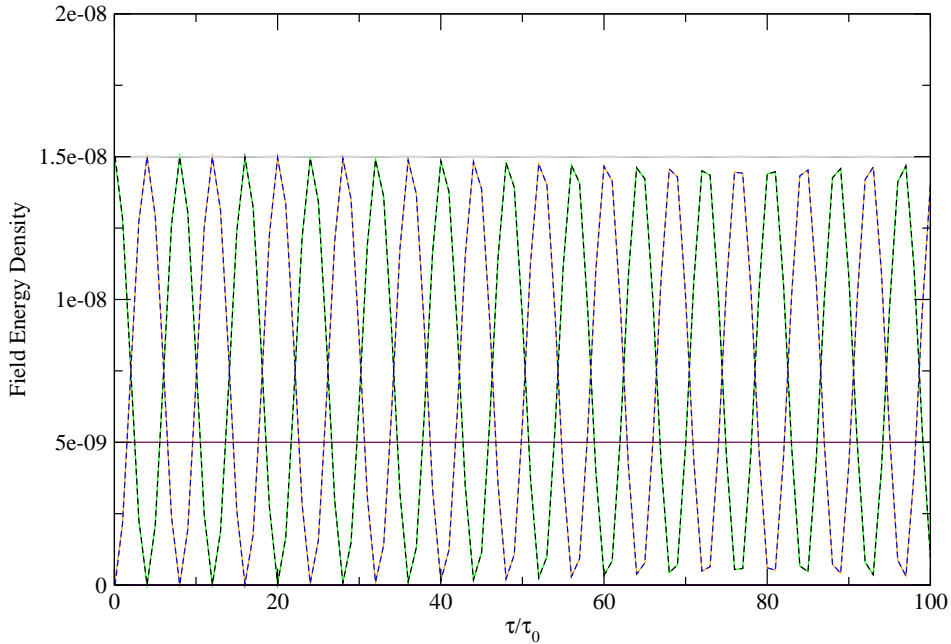


Figure 4: The proper-time dependence of the chromo-field energy densities resulting from a stationary run with a single non-Abelian mode along the eta direction without coupled currents. Run was made using $\tau_{\text{iso}} = 1.0$, $\tau_0 = 1.0$, $m_D = 10$, $\sigma = 10^{-4}$, $a = 1.00$, $a_\eta = 1.00$, $\epsilon = 0.1$, $N_\eta = 16$, $N_x = 16$, $N_u = 8$ and $N_\phi = 8$.

dashed lines are given by the new codebase where as the continuous lines are all from a stationary independent “hal” code. As one can easily make out the curves lie just on top of each other. The vertical lines is the unchanged gain rate due to uncoupled currents. A second physical testcase involved a comparison with the HEL 1d code with longitudinal nodes without transversal effects. As expected it worked for the early time evolution.

3.3 Preliminary results

As expected the 3d code versus the already performed 1d simulation demands much more memory and time. The run in Fig (5) is done on a crude and quick lattice to get some intuition about the field energy density evolution.

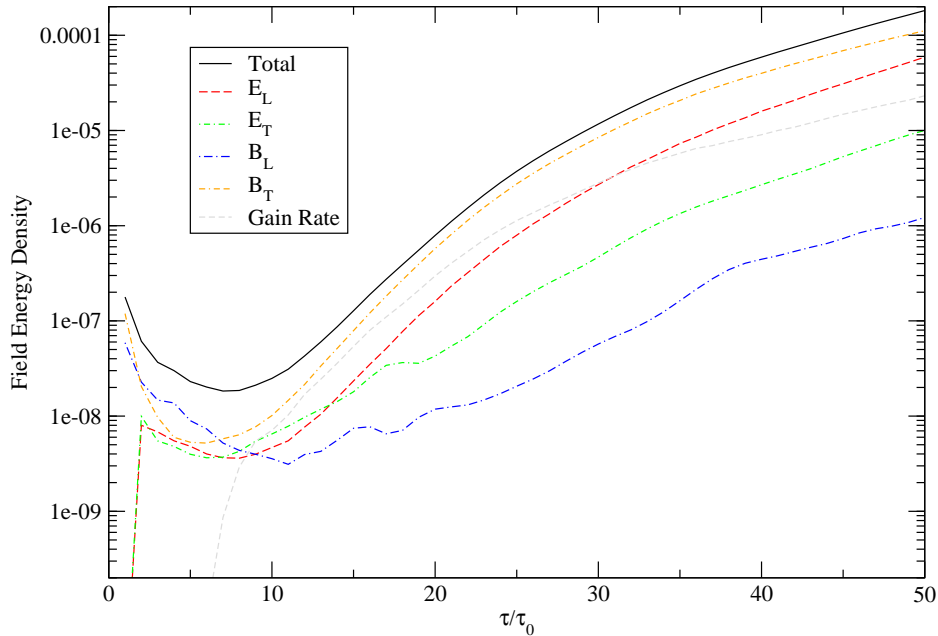


Figure 5: The proper-time dependence of the chromo-field energy densities resulting from a run with a single non-Abelian mode Run was made using $\tau_{\text{iso}} = 1.0$, $\tau_0 = 1.0$, $m_D = 10$, $\sigma = 10^{-4}$, $a = 1.00$, $a_\eta = 1.00$, $\epsilon = 0.1$, $N_\eta = 16$, $N_x = 16$, $N_u = 8$ and $N_\phi = 8$.

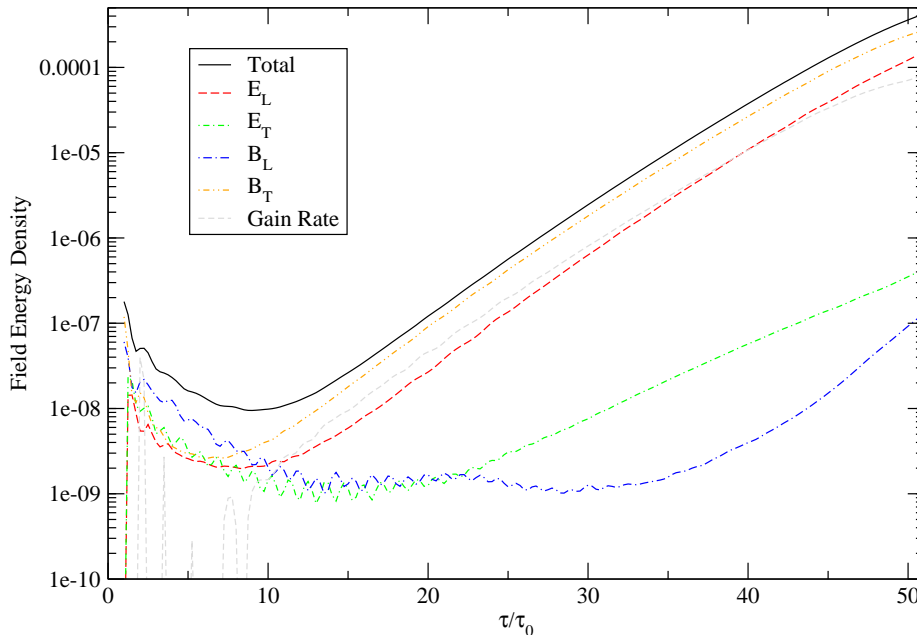


Figure 6: The proper-time dependence of the chromo-field energy densities resulting from a run with a single non-Abelian mode Run was made using $\tau_{\text{iso}} = 1.0$, $\tau_0 = 1.0$, $m_D = 10$, $\sigma = 10^{-4}$, $a = 1.00$, $a_\eta = 1.00$, $\epsilon = 0.025$, $N_\eta = 16$, $N_x = 16$, $N_u = 128$ and $N_\phi = 16$.

4 Conclusion and Outlook

Non-Abelian plasma instabilities play a crucial role in the nonequilibrium dynamics of a weakly coupled quark-gluon plasma. We have started to work out the dynamics of the most unstable modes in the transverse direction in full 3+1-dimensional configuration space and momentum space. The evolution of plasma instabilities is affected by two competing effects: the density of the plasma is decreasing with time and so is the growth rate of the instabilities, the increase of the momentum-space anisotropy however leads to more unstable modes.

We thus conclude that non-Abelian plasma instabilities show rich physics in real time HEL lattice evolutions.

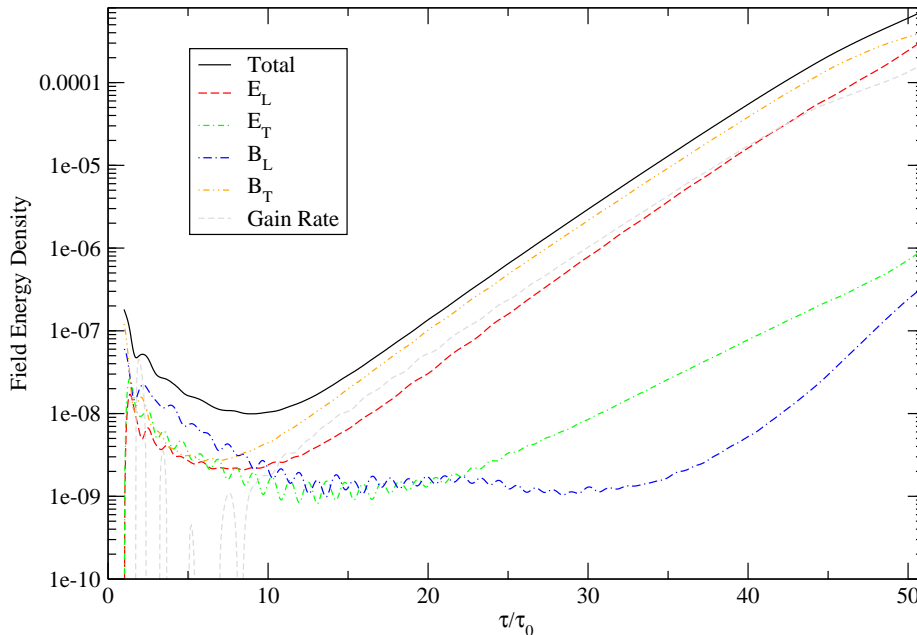


Figure 7: The proper-time dependence of the chromo-field energy densities resulting from a run with a single non-Abelian mode Run was made using $\tau_{\text{iso}} = 1.0$, $\tau_0 = 1.0$, $m_D = 10$, $\sigma = 10^{-4}$, $a = 1.00$, $a_\eta = 1.00$, $\epsilon = 0.005$, $N_\eta = 16$, $N_x = 16$, $N_u = 64$ and $N_\phi = 16$.

As an outlook we will calculate bigger lattices with many \mathcal{W} fields on small time steps based on the HEL 3 dimensional code and expect to incorporate several different possible initial conditions. In future work we intend to carry out full 3+1 dimensional simulations running on the super computer the Vienna Scientific Cluster using a MPI parallellized code version.

5 Personal Experience

The numerical studies have deepened and honed my skills in programming large scale problems in C/C++. I also got introduced into programming Message Passing Interface (MPI) for high-performance parallel computing. I gained lots of insights on the physics of the QGP in several dense discussions and resulting calculations. I immensely profited from the focused work environment at the Gettysburg College. My own personal experience got highly enriched thanks to the contact with the American culture.

A Academic life in Gettysburg College and advises for later successors

The Gettysburg College, located on a charming campus near the famous battlefield, teaches around 2600 students employing more than 190 faculty members. It features impressive sports facilities (swimming pool, tennis courts, athletic complex, indoor climbing wall, ..). The Gettysburg College administration kindly allowed full participation in faculty events like the “Friday Faculty Luncheon” (Lunch And Talk) or the “Friday Afternoon Social Hour” (FASH) and in any sports program of “Center for Athletics, Recreation, and Fitness”. Shortterm rents, although not too expensive, are rare and thus hard to find in Gettysburg. The College is best reached by the College transportation vans from Washington International Airport for a transportation fee.

The fancy footwork a J1 Visa sponsored is done via the “Lutheran Evangelical Student Association”. One has to be prepared to get constraint to an expensive health insurance for the total stay. It is advisable to stay in the US for the whole duration of the J1 visa. As the rules of the J1 visa might be interpreted in stronger terms than official documents indicate an eventual visit to neighbouring Canada might not be waved.

The capital of the United States Washington, DC is only approximately 2 driving hours away. The free visits of the National Mall with the very impressive “National Gallery of Art” and “National Museum of Natural History” is highly recommended. New York City, a global center with many important international influences is about 5 driving hours away. The “Appalachian National Scenic Trail” which stretches through Pennsylvania across “Michaux State Forest” near Fuller lake can be explored with the famous American Trek mountainbikes thanks to the excellent “Gettysburg Bicycle and Fitness” shop. The “Gettysburg Pirate Orchestra”, a charming band of instrument-playing professors and townsfolk, introduces Blue Grass, Americana, Folk, and Pop to enthusiastic audiences in all the different Gettysburg Coffey places like “Ragged Edge” or “Garryowen Irish Pub”. A tour of the historic battle field is best done early in the year before the tourist seasons kicks in and the various reenactment plays.

References

- [1] E. V. Shuryak, World Sci. Lect. Notes Phys. **71**, 1 (2004) [World Sci. Lect. Notes Phys. **8**, 1 (1988)].
- [2] M. J. Tannenbaum, “Recent results in relativistic heavy ion collisions: From ‘a new state of matter’ to ‘the perfect fluid’”, *Rept. Prog. Phys.* **69**, 2005 (2006).
- [3] P. Romatschke and U. Romatschke, Phys. Rev. Lett. **99**, 172301 (2007) [arXiv:0706.1522 [nucl-th]].
- [4] P. B. Arnold, Int. J. Mod. Phys. E **16**, 2555 (2007) [arXiv:0708.0812 [hep-ph]].
- [5] S. Mrówczyński, “Stream instabilities of the quark-gluon plasma”, *Phys. Lett.* **B214**, 587 (1988).
- [6] S. Mrówczyński, “Plasma instability at the initial stage of ultrarelativistic heavy ion collisions”, *Phys. Lett.* **B314**, 118 (1993).
- [7] Y. E. Pokrovsky and A. V. Selikhov, “Filamentation in a quark-gluon plasma”, *JETP Lett.* **47**, 12 (1988).
- [8] B. Schenke and M. Strickland, “Fermionic collective modes of an anisotropic quark-gluon plasma”, *Phys. Rev.* **D74**, 065004 (2006).
- [9] P. Romatschke and A. Rebhan, “Plasma instabilities in an anisotropically expanding geometry”, *Phys. Rev. Lett.* **97**, 252301 (2006).
- [10] A. Rebhan, M. Strickland and M. Attems, Phys. Rev. D **78**, 045023 (2008) [arXiv:0802.1714 [hep-ph]].
- [11] S. Mrowczynski, Acta Phys. Polon. B **37**, 427 (2006) [arXiv:hep-ph/0511052].
- [12] S. Mrowczynski, A. Rebhan and M. Strickland, Phys. Rev. D **70**, 025004 (2004) [arXiv:hep-ph/0403256].
- [13] A. Rebhan, P. Romatschke and M. Strickland, JHEP **0509**, 041 (2005) [arXiv:hep-ph/0505261].